Desensitization to commodity price fluctuations by product characteristics

Keiji Sakakibara[1] and Daniel M. Packwood[2,*]

[1]*Graduate School of Advanced Integrated Studies in Human Survivability (GSAIS), Kyoto University, Kyoto 606-8306, Japan*

[2]*Institute for Integrated Cell-Material Sciences (iCeMS), Kyoto University, Kyoto 606-8302, Japan*

(Received 8 May 2024; accepted 6 August 2024; published 3 September 2024)

Little is known about how commodity price fluctuations transmit to the prices of products. In this paper we present a price dynamics model for a product which is in competition with a commodity. The price of the commodity is treated as a stochastic process. Commodity price fluctuations are transmitted to the product price through a demand function which is obtained by aggregating the choices of a consumer population. Importantly, these consumers make their choices on the basis of a utility function which includes a term relating to product characteristics. Numerical simulations show that improved product characteristics tend to suppress the transmission of commodity price fluctuations. We apply our model to a realistic case of monolayer platinum (a product) in competition with platinum metal (a commodity) for adoption by consumers as a catalyst material. While monolayer platinum shows only a minor improvement in catalytic turnover rates for oxygen reduction, the resulting product characteristic improvement is sufficient to effectively eliminate product price fluctuations, at least for the consumer population regime considered here.

DOI: 10.1103/PhysRevE.110.034106

I. INTRODUCTION

Price fluctuations are of considerable interest to econophysics. Two lines of research in this direction can be identified. One line of work aims to model price fluctuations by characterizing the underlying stochastic dynamics and building appropriate generating equations [1–4]. The other aims to explain the emergence of price fluctuations by building microscopic agent-based models for the consumers and suppliers [5–7]. Regardless of which approach is taken, any realistic price model should consider how prices of different products and commodities are affected by each other. Correlations between prices in financial markets are well established [8,9] and almost certainly exist in other markets as well. At present, our understanding of how price fluctuations are transmitted between products on a microscopic level is incomplete, and the factors which modulate this transmission are poorly understood.

To clarify, let us consider a situation where a product competes with a commodity for selection by consumers in a particular market. Such a situation might occur in the chemical industry. For example, ethanol (a commodity chemical) competes with chlorhexidine (a product chemical) for selection by the producers of antiseptic solutions (for example, see [10]). Polyethylene (a commodity) competes with various speciality polymers such as polytetrafluoroethylene for selection in certain applications [11]. Moreover, novel solid-state materials (products) often compete with precious metals (commodities) for adoption as catalytic materials in fuel cells [12]. In such situations, it is clear that fluctuations in the commodity price must be transmitted to the price of the competing product. Indeed, strong upward fluctuations in the commodity price will tend to push consumers towards the competing product, causing an upward shift in the price of the product through a sudden demand shock. The reverse will happen when the commodity price undergoes a strong downward fluctuation. While common sense, this phenomenon is not easy to model on a microscopic level.

Moreover, there is another aspect to the problem that has received little attention: the role played by product characteristics. In order to be adopted by consumers, products need to have superior characteristics compared to the competing commodity. Returning to the above example, monolayer platinum (a novel solid-state material) could potentially displace platinum metal (a commodity) in fuel cell technologies due to its superior catalytic turnover rate for oxygen reduction [13]. In this example, the relevant product characteristics can be identified with catalytic reaction rates; in general, the relevant product characteristics will be the ones deemed important by the consumers in the specific market. Stated in general terms, the problem that we wish to study is as follows: how do product characteristics affect the transmission of commodity price fluctuations to the prices of those products? At present, the tools of econophysics offer little insight into such questions.

The effect of product characteristics has received considerable attention within mainstream economics, although not from the perspective of price dynamics. In classical economics research, the effect of product characteristics is investigated as a revealed preference problem, in which consumers reveal their attitudes towards product characteristics through their consumption choices (see [14] for a discussion). In modern microeconomics, product characteristic terms are directly embedded into the utility functions of individual consumer units, from which (equilibrium) expressions for price are deduced from an aggregate demand function [15–17].

*Contact author: dpackwood@icems.kyoto-u.ac.jp

The latter approach seems most amenable to the approaches used in econophysics, in which equations of motion for prices are sought by deriving expressions for demand and supply. Like establishing a micro-macro correspondence in statistical mechanics on the basis of a Hamiltonian function, understanding the effects of product characteristics on price fluctuations requires establishing a correspondence between individual consumer units and market prices on the basis of a utility-derived demand function.

In this paper we present a price dynamics model for the situation described above. Concretely, we consider the case of a product competing in a market with a commodity whose price follows a stochastic process. An expression for product demand is derived from a microscopic model of consumers, who make their consumption choices on the basis of a utility function which incorporates a term related to product characteristics. The resulting demand function resembles a sigmoidal activation function of the type which appears in the study of neuron dynamics [3,18,19] and serves to transmit commodity price fluctuations to the price of the competing product. We further find that improved product characteristics tend to desensitize the product price to commodity price fluctuations. This is confirmed through numerical simulations, which also show that such desensitization is strongly conditional on the state of the market. In particular, desensitization is not guaranteed when consumers are highly uniform in their preferences towards good product characteristics. Finally, we apply our model to the case of a monolayer catalyst in competition with pure platinum, using density functional theory (DFT)-calculated catalytic turnover rates as a measure of catalyst quality. While these calculations predict only a minor lowering of activation energy for oxygen reduction on monolayer platinum compared to pure platinum, subsequent numerical simulations show that the resulting improvement in product characteristics is sufficient to essentially eliminate price fluctuations, at least under the market conditions that we consider. This paper therefore provides understanding about how price fluctuations are transmitted between products on a microscopic level, and how such transmission can be modulated by product characteristics.

This paper is organized as follows. In Sec. II we introduce our model and derive an expression for the demand function from microscopic considerations. In Sec. III, we present numerical simulation results of our model for two cases: where the commodity price follows an Ornstein-Uhlenbeck process, and where the commodity price is simulated from a time-series model fitted to real platinum price data. The latter part of Sec. III also presents our DFT calculations of oxygen reduction turnover rates on monolayer platinum and pure platinum catalysts, which are used to measure product characteristics. Discussion and conclusions are left to Secs. IV and V.

II. PRICE DYNAMICS MODEL

Consider a market of N consumers and two items: a commodity C and a product M which can be produced cheaply. Our model makes five basic assumptions: (i) at each point in time, each consumer purchases exactly one unit of either M or C; (ii) consumer choices are Markovian, in the sense that they depend only upon current prices (as well as other model parameters); (iii) the price p_M of M follows

$$\frac{dp_M}{dt} = -\gamma(S_M - D_M), \tag{1}$$

where S_M is the supply of M, D_M the demand, and $\gamma > 0$ is a constant; (iv) the supply of M is given by

$$S_M = a + bp_M, \tag{2}$$

where $a, b > 0$ are constants; and (v) the price p_C and supply of C are unaffected by demand fluctuations in this market. Assumptions (i) and (ii) simplify the calculation of the demand function. Assumption (v) implies that C is traded in very many markets simultaneously and is therefore negligibly influenced by the conditions of the specific market considered in the market. This is analogous to the assumption of "no reactive feedback" from the system to the surroundings used in stochastic models in statistical physics [20]. In contrast, assumption (iii) implies that M is only traded in the specific market considered by the model, and hence is strongly affected by its market conditions.

We derive an expression for the demand of M by aggregating the decisions of each consumer in the market. Thus, let u_{ki} denote the marginal utility gain for consumer k upon selecting item i ($i \in \{M, C\}$). Suppose that

$$u_{ki} = \beta_k \ln W_i - \alpha_k p_i, \tag{3}$$

where $\beta_k \geqslant 0$ and $\alpha_k \geqslant 0$ are constants, and W_i denotes the product characteristic for item i. In general, W_i will be determined by the aspect of the product which is deemed most important by the consumers in the market under consideration. For the case of a market of chemical engineers, where C and M might be used as catalysts for a particular chemical reaction, W_i might denote catalytic turnover rate. The logarithm implies diminishing utility gains with improving product characteristics, which is consistent with treatments of product characteristics used in mainstream economics [15]. The coefficients β_k and α_k measure the importance that consumer k places on the product characteristic and price, respectively, when making their decision. According to Eq. (3), consumer k will purchase C if and only if $u_{kC} > u_{kM}$. Inserting Eq. (3) into this inequality and rearranging yields

$$\frac{\beta_k}{\alpha_k} < B = \frac{p_M - p_C}{Q}, \tag{4}$$

where we have assumed that $W_C < W_M$. In the above, Q is the *log characteristic ratio*, defined as $Q = \ln W_M/W_C$. For a fixed instance of the prices p_M and p_C, the demand for C is therefore

$$D_C(p_M, p_C) = \sum_{k=1}^{N} \mathbf{1}\left(\frac{\beta_k}{\alpha_k} < B\right), \tag{5}$$

where $\mathbf{1}$ denotes the indicator function. The demand for M is simply

$$D_M(p_M, p_C) = N - \sum_{k=1}^{N} \mathbf{1}\left(\frac{\beta_k}{\alpha_k} < B\right). \tag{6}$$

In order to transform Eq. (6) into a form more useful for calculations, we assume that $\beta_1, \beta_2, \ldots, \beta_N$ and $\alpha_1, \alpha_2, \ldots, \alpha_N$

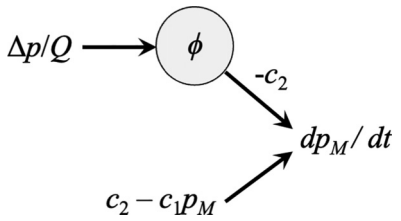

FIG. 1. Diagrammatic representation of the price dynamics model [Eq. (10)]. See Sec. II for details

are sequences of independent and identically distributed random variables. Let Pr denote probability and observe that $\Pr(\beta_k/\alpha_k < B)$ is independent of k. By the law of large numbers, we therefore have that

$$D_M(p_M, p_C)/N \to 1 - \phi(B) \tag{7}$$

with probability 1 as N goes to infinity, where ϕ is the cumulative distribution of the random variable β_k/α_k.

A renormalization argument is required in order to write our final evolution equation for the price. We let $\gamma \to 0$ as $N \to \infty$ such that

$$\gamma b = c_1 \tag{8}$$

and

$$\gamma N = c_2, \tag{9}$$

where c_1 and c_2 are positive constants. The condition in Eq. (8) implies that the supply curve for M is highly elastic, meaning that that supply adjusts readily to changes in the price of M. On the other hand, the condition $\gamma \to 0$ implies that we are considering a highly damped situation in which prices are extremely "sticky" and adjust slowly. This might occur when wages and other outlays for the production of M are slow to adjust to market conditions. Utilizing these conditions and inserting Eqs. (2) and (7) into Eq. (1) yields

$$\frac{dp_M}{dt} = -c_1 p_M + c_2[1 - \phi(B)], \tag{10}$$

where we have allowed $\gamma a \to 0$ for simplicity. The time evolution of p_M is coupled to p_C through the function ϕ, as can be seen by writing B explicitly:

$$B = \frac{\Delta p}{Q}, \tag{11}$$

where $\Delta p = p_M - p_C$ denotes the price difference between M and C.

Equations of the form of Eq. (10) are widely used to model neuron firing dynamics [3,18,19]. In these cases, the sigmoidal function ϕ is referred to as the activation function. While this connection is purely coincidental, it is convenient to refer to ϕ as an activation function in the present case as well, and to represent Eq. (10) diagrammatically as a neuron model. Such a representation is shown in Fig. 1. The "neuron," corresponding to the activation function, receives an input signal $\Delta p/Q$. The output signal of the neuron is then added to another signal $c_2 - c_1 p_M(t)$, resulting in the final output $dp_M(t)/dt$. It is through the activation function that the fluctuations in the commodity price are transmitted to the price of the product. We will use this diagrammatic representation of the model to facilitate discussions in the following sections.

TABLE I. Parameters used for the case of Gaussian commodity. h is the time step, and n_{ts} is the number of time steps. Other parameters are defined in the text.

c_1	0.1	v_a	0.75
c_2	0.3	v_b	0.75
W_C	1.0	τ	5.0
W_M	1.25	c	1.5
μ_a	1.0	h	10^{-4}
μ_b	2.5	n_{ts}	10^6

III. NUMERICAL SIMULATIONS

We perform simulations for two cases. For the first case ("Gaussian commodity"), we suppose that p_C is an Ornstein-Uhlenbeck process following the stochastic differential equation:

$$\frac{dp_C}{dt} = -\frac{1}{\tau} p_C + c^{1/2} F(t), \tag{12}$$

where τ and c are positive constants and $F(t)$ is Gaussian white noise with mean zero, unit variance, and correlation function $\langle F(t)F(t')\rangle = \delta(t - t')$, where $t > t'$. The Ornstein-Uhlenbeck process is chosen as a generic stochastic process for commodity price evolution and is sufficient for illustrating the key behavior of our price dynamics model. Indeed, we will obtain our conclusions entirely on the basis of the "neuron" representation of the model above without referring to the distributional properties of p_C. For the second case ("platinum commodity"), we consider the case of a realistic product in which M is a monolayer platinum catalyst and C pure platinum, and p_C is generated according to a time-series model fitted to a real platinum price data. Moreover, a realistic value of the parameter Q is calculated using density functional theory calculations, as described later. The main purpose of this second case is therefore to illustrate some possible behavior of p_M given a realistic value of Q for real materials.

For expediency, we assume that $\alpha_k \sim N(\mu_a, \sigma_a^2)$ and $\beta_k \sim N(\mu_b, \sigma_b^2)$, respectively, where N is the normal distribution. Under this assumption, the distribution of β_k/α_k is approximately normal with mean

$$\mu = \mu_b/\mu_a \tag{13}$$

and variance

$$\sigma^2 = \mu^2\left(v_a^2 + v_b^2\right), \tag{14}$$

where $v_a = \sigma_a/\mu_a$ and $v_b = \sigma_b/\mu_b$ are the coefficients of variation for α_k and β_k, respectively [21]. μ measures the degree to which the average consumer values characteristics over price. σ measures the degree of heterogeneity in consumer preferences as a fraction of μ. Note that the above approximation is reliable only when the coefficients of variation are suitably small (less than unity).

Unless otherwise mentioned, all simulations used the parameter settings listed in Table I. These include two supply-side parameters (c_1 and c_2) and four consumer-side

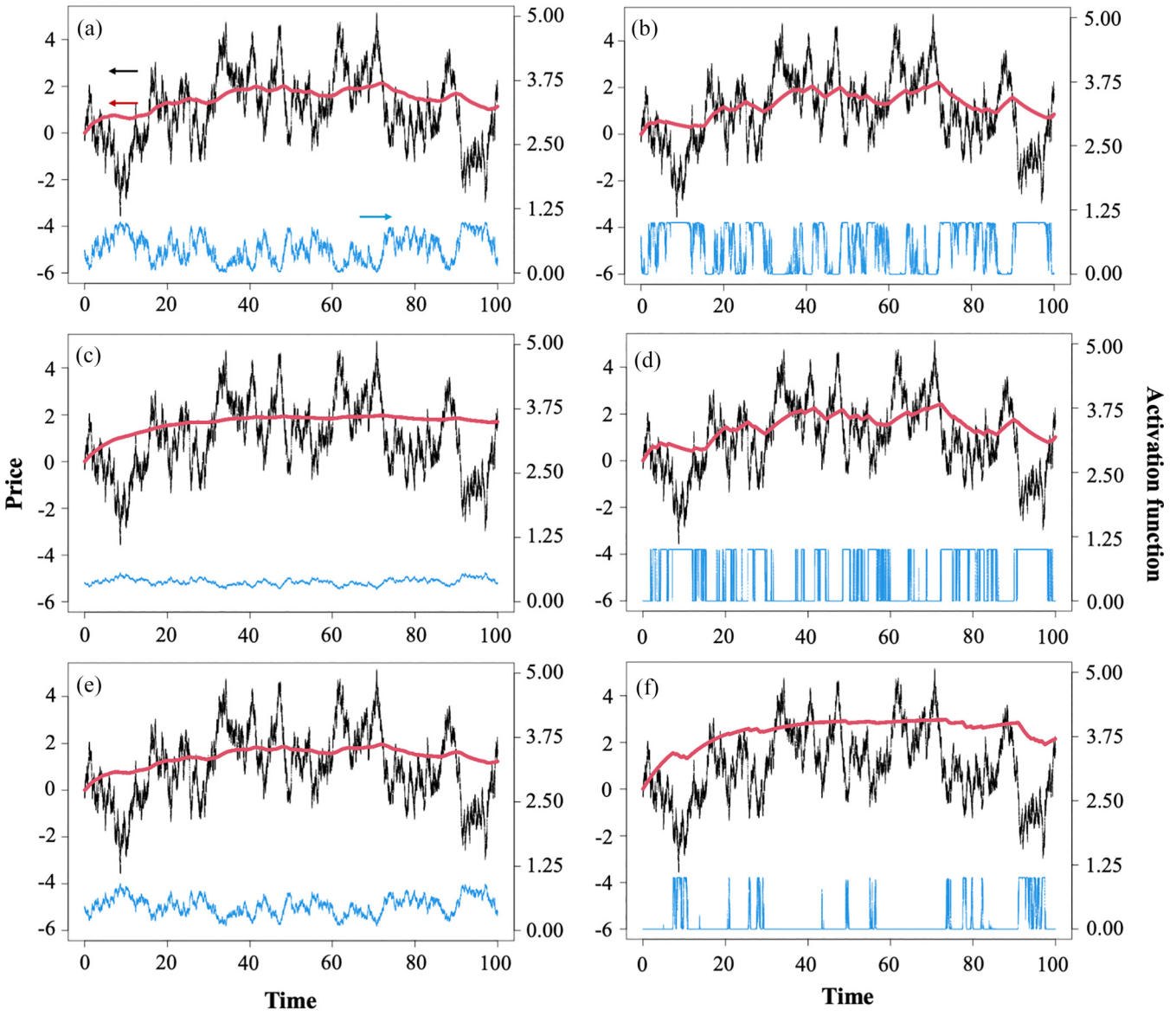

FIG. 2. Representative price trajectories for the Gaussian commodity case. Red curve is p_M, black curve is p_C, and blue curve is the activation function. (a) Baseline case; (b) small log characteristic ratio case ($W_M/W_C = 1.05$); (c) large log characteristic ratio case ($W_M/W_C = 3.50$); (d) low consumer heterogeneity case ($v_a = 0.1$, $v_b = 0.1$); (e) high consumer heterogeneity case ($v_a = 1.0$, $v_b = 1.0$); and (f) high log characteristic ratio, low consumer heterogeneity case ($W_2 = 3.50$, $v_a = 0.1$, $v_b = 0.1$). Unless otherwise mentioned, all parameters set as in Table I.

parameters (μ_a, μ_b, v_a, and v_b). Our choices of c_1 and c_2 imply that $b/N = 1/3$, according to Eqs. (8) and (9). This means that a unit increase in product prices induces suppliers to increase aggregate supply of M by one-third the number of potential consumers. This is reasonable, as under the assumptions of the model we would expect b/N to be positive but less than 1 (since there would be no reason to produce more product than the number of potential sales). The parameters μ_a and μ_b describe the preferences of the average consumer in the population. Differentiating the utility expression in Eq. (3) and averaging over all consumers yields $du_i = \mu_b dW_i/W_i - \mu_a dp_i$, where u_i is the marginal utility gain of the average consumer upon selecting i. Thus, our choices of $\mu_a = 1.0$ and $\mu_b = 2.5$ imply that the average consumer gains 2.5 times as much benefit from a percentage improvement in product characteristic (dW_i/W_i) compared to a unit reduction in price. This is reasonable: within the assumptions of the model, all consumers have already committed themselves to purchasing one of the two items and must therefore have a particular need for the characteristics of these items. For these consumers, price should be a secondary consideration. The setting of $v_a = 0.75$ and $v_b = 0.75$ is reasonable as well. In other studies, coefficients of variation for similar parameters are typically between 0.1 and 0.6 when measured from consumption data, exceeding 1.0 slightly for extreme cases [15,22].

A. Gaussian commodity case

Representative price trajectories for the Gaussian commodity case are presented in Fig. 2. These trajectories were

obtained by integrating the price equation [Eq. (10)] using the Euler-Maruyama algorithm with a time step of 10^{-4} units [note that the Euler-Maruyama algorithm is not necessary, as Eq. (10) does not contain any stochastic differentials]. The Gillespie algorithm was used to propagate p_C [23]. Figure 2(a) shows the case where the baseline parameters from Table I were used for the simulation. The thick red, black, and blue curves correspond to p_M, the fluctuating commodity price p_C, and the value of the activation function, respectively. It can be seen that p_M fluctuates less violently than the incoming stochastic input p_C, despite obvious fluctuations in the activation function. This is expected in the overdamped regime considered by the model, where prices become sticky. Nonetheless, p_M displays a high degree of irregularity. Indeed, p_M appears to rise when p_C is larger than p_M, and appears to fall when p_C is smaller than p_M. This is expected for the reasons mentioned earlier: upward fluctuations in the commodity price will push consumers towards the competing product M, causing a the price of M to rise due to increased demand, and conversely for downward fluctuations. Our model therefore transmits commodity price fluctuations to the product price in a sensible manner.

We now consider the case where the log characteristic ratio Q is very small [Fig. 2(b)]. Concretely, we set W_M/W_C to 1.05, which yields $Q = 0.05$. For this case, it can be seen that the activation function value evolves in a way somewhat reminiscent of telegraph noise, spending most of its time in one of two states (1 or 0). This behavior can be anticipated from the diagrammatic representation in Fig. 1, which shows when Q is small, the input signal $\Delta p/Q$ is extremely sensitive to small changes in the price difference. Suppose that the price difference is suitably large, such that the right-hand asymptotic tail of the activation function is being probed by the input signal. At this instance, $\phi(B)$ is essentially 1. As the price difference decreases, the highly sensitive input signal will shoot past the sigmoidal inflection point of the activation function and end up probing the left-hand asymptotic tail, where $\phi(B)$ is essentially 0. As the price difference increases again, the input signal will again shoot past the inflection point, and end up probing the right-hand asymptotic tail once more. This accounts for the telegraph noiselike behavior of the activation function when Q is very small. The transition between 0 and 1 occurs as the input signal sweeps through the inflection point, which occurs when $B = \mu$, or equivalently when $p_M - p_C = Q\mu \approx 0$. Indeed, it can be seen that the transitions in the activation function tend to occur when trajectory of p_M (the red line) intersects with the trajectory of p_C (the black line).

What remains to be explained is the smooth rise and decay of p_M between transitions of the activation function. It can be seen that p_M tends to decrease when the activation function is close to 1 (when the input signal probes the right-hand asymptotic tail). Conversely, p_M tends to increase when the activation function is residing at 0. Both behaviors are expected on intuitive grounds: the input signal probes the right-hand asymptotic tail when Δp is suitably large, which implies that the product price is high compared to the commodity price, and hence that demand for the product is decreasing. The converse explanation holds when the input signal probes the left-hand asymptotic tail. Moreover, both behaviors can be readily explained by inspecting our price evolution equation [Eq. (10)]. Indeed, when $\phi(B) = 1$, the price evolution equation reduces to $dp_M/dt = -c_1 p_M$, which yields damped dynamics. When $\phi(B) = 0$, the price evolution equation becomes $dp_M/dt = -c_1 p_M + c_2$. This equation describes dynamics of the form $p_M = [c_2 - \exp(-c_1 t)]/c_1$, which describes a smooth, nonlinear rise with an asymptotically constant value. While mathematically nonrigorous, this analysis qualitatively explains the behavior observed when the log characteristic ratio Q is very small.

Reexamining the baseline case [Fig. 2(a)], similar features to those identified above can be discerned. While the activation function evolves in a decidedly different manner from the telegraph noise-type process described above, the price p_M displays similar evolution. It tends to decrease when the activation function is near 1, increase when the activation function is near zero, and undergo transitions whenever the trajectory of p_M intersects the trajectory of p_C. Between transitions, p_M appears to undergo a smooth evolution. While quantitatively different, it appears that both the baseline case and the small-Q case can be qualitatively understood in terms of a similar picture: that of an input signal $\Delta p/Q$ sweeping back and fourth through the activation function, changing the direction of the trajectory of p_M whenever it passes through the sigmoidal inflection region.

We now consider the case where the Q is large [Fig. 2(c)]. We set W_M/W_C to 3.50, which yields $Q = 1.26$. Under these conditions, the input signal $\Delta p/Q$ is relatively insensitive to changes in the price difference, and will spend more time probing the activation function in the region of the sigmoidal inflection point as a result. This is evident from the blue line in Fig. 2(c), which shows a relatively stable evolution for the value of the activation function. As a result, the evolution of p_M becomes remarkably steady. While the direction of the p_M trajectory again appears to change whenever it intersects the p_C trajectory, the overall degree of fluctuation remains negligible. Taken together, these results show that poor improvements in characteristics compared to the commodity lead to unstable and irregular product price dynamics, whereas large improvements tend to reduce product price fluctuations by suppressing the transmission of commodity price fluctuations.

We now turn to the effect of consumer population characteristics on price dynamics. The two relevant parameters are μ and σ, which describe the preferences of the average consumer and the variation of preferences across the population as a whole, respectively. In our framework it is not possible to vary μ without affecting σ [as is evident from Eq. (14)]. We will therefore vary the values of v_a and v_b, the coefficients of variation for product price preferences and characteristic preferences, while holding μ constant. Figure 2(d) shows the case where v_a and v_b are small ($v_a = 0.1$, $v_b = 0.1$). The result strongly resembles the case of small Q, although now the telegraph noiselike evolution of the activation function is even more pronounced. This result can be explained using similar ideas to those developed above. When the coefficients of variation are particularly small, the activation function resembles a step function with the inflection region tightly localized at the point μ. If the input signal $\Delta p/Q$ is small but tending to increase, it will eventually pass through the step region, where

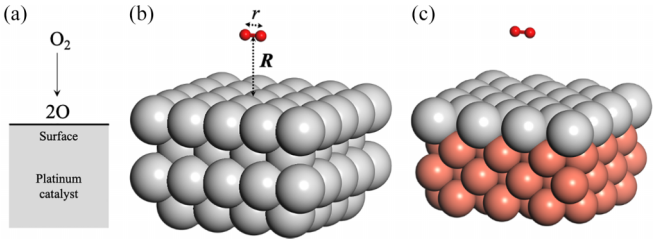

FIG. 3. (a) Illustration of oxygen splitting by a platinum catalyst used in fuel cells. (b) Slab model a platinum catalyst (Pt catalyst) system used in this study. Gray and red spheres represent platinum and oxygen atoms, respectively. The red bar connecting the two oxygen atoms represents the chemical bond in the oxygen molecule. R is the height of the oxygen molecule with respect to the catalyst surface, and r is the oxygen bond length. (c) Slab model of a monolayer platinum catalyst (M-Pt catalyst). Copper atoms are represented by brown-orange spheres. Slab models drawn with the Materials Studio Visualizer software [24].

the activation function will abruptly change its value from 0 to 1. The opposite will happen if $\Delta p/Q$ is large but tending to decrease. The same arguments developed above can then be applied to explain the unstable and irregular trajectory for p_M, which bears a striking resemblance to the one in Fig. 2(b).

Figure 2(e) shows the case where v_a and v_b are large ($v_a = 1.0$, $v_b = 1.0$). In this case, the activation function trajectory is relatively stable, fluctuating in an unremarkable way about the value $1/2$. When the coefficients of variation are large, the inflection region of the activation function broadens, approximating a horizontal line over a wide range of values. As a result, the activation function becomes more insensitive to the input signal. The price trajectory for p_M therefore becomes stable, and the transmission of commodity price fluctuations to the product price becomes ineffective.

These results therefore demonstrate two ways in which the transmission of commodity price fluctuations can be suppressed: through large improvements in characteristics of the product relative to the commodity, or through a strong heterogeneity in consumer tastes. Both of these conditions appear necessary in order to stabilize price fluctuations. Figure 2(f) shows results for the case of large log characteristic ration and low consumer heterogeneity ($Q = 1.26$, $v_a = 0.1$, $v_b = 0.1$). While less dramatic than the small-Q case [Fig. 2(b)], the price trajectory for p_M still shows significant stochastic fluctuations. This indicates that large improvements in product characteristics might not be enough to desensitize prices to commodity price fluctuations, especially when consumer preferences are relatively homogenous across the population.

B. Platinum commodity case

We now consider a more concrete situation shown in Fig. 3, which shows two materials which catalyze the oxygen splitting reaction ($O_2 \rightarrow 2O$, Fig. 3(a)]. This reaction is of critical importance in hydrogen fuel cells [12], where high reaction rates are required to ensure efficient energy generation. Figure 3(b) shows a pure platinum (Pt) catalyst, which is widely used in commercial hydrogen fuel cells at present. While a highly effective catalyst, Pt is an expensive commodity which is subject to unpredictable price fluctuations. Figure 3(c) shows an alternative catalyst that might serve as a replacement for Pt in fuel cell technologies. This catalyst, which we denote M-Pt, consists of a platinum monolayer supported on a copper substrate. Other types of monolayer catalysts have been proposed previously [13]. In terms of the model described above, Pt would act as the commodity C, and M-Pt as the competing product M. This correspondence is possible due to the negligible price of copper compared to platinum, the negligible amount of platinum used in the production of M-Pt, as well as the fact that M-Pt and Pt would be competing for the same consumers in certain markets (such as fuel cell producers). We wish to compute the log characteristic ratio Q between M-Pt and Pt and determine whether the price of M-Pt can be desensitized to fluctuations in the price of platinum.

For the case of catalytic materials, the product characteristics can be set equal to the rate constant for O_2 dissociation, which is given by the Arrhenius equation:

$$W_i = A_i \exp\left(-\frac{\epsilon_i}{k_B T}\right), \tag{15}$$

where i denotes either M-Pt or Pt, k_B is the Boltzmann constant, T is the temperature, A_i is the frequency factor, and ϵ_i is the activation energy. We can assume that the frequency factors A_i are independent of catalyst type, since both catalysts should involve similar reaction geometries. The log characteristic ratio $Q = \ln W_{\text{M-Pt}}/W_{\text{Pt}}$ then reduces to

$$Q = -\frac{\epsilon_{\text{M-Pt}} - \epsilon_{\text{Pt}}}{k_B T}. \tag{16}$$

The activation energies are computed using density functional theory (DFT) using slab models for the M-Pt and Pt catalysts. DFT is a well-established method for solving the Schrödinger equation for systems of electrons in solid materials and molecules (see [25,26] for reviews). The following calculations follow those presented in Refs. [13] and [27], which also applied DFT to monolayer catalysts. The M-Pt slab was first generated by creating a three-layer Cu slab terminated at the 001 face and placing Pt atoms on top of the hollow positions. The Pt catalyst structure was generated using a four-layer Pt slab terminated at the 001 face. We consider the 001 faces, as these are known to be the preferred face for O_2 dissociation for platinum [27]. The slab dimensions were 10.84×15.35 Å for M-Pt and 11.10×11.10 Å for Pt. The slabs were relaxed using DFT with the bottom two atom layers kept frozen. Relaxation was performed as implemented in VASP version 5.4.4 [28], using the PBE exchange-correlation function [29], PAW-PBE pseudopotentials, a 450 eV basis set cutoff, and $1 \times 1 \times 1$ Γ-centered k-point grids.

To obtain the activation energy, an O_2 molecule with a bond length r was placed at various heights R above the M-Pt or Pt slab, in such a way that the O-O bond was parallel to the surface and intersected midway through one Pt-Pt bond [see Fig. 3(b)]. For given values of r and R, the energy of interaction between the O_2 molecule and the catalyst slab was calculated according to the formula

$$E_{\text{int}}(r, R) = E(r, R) - E_{\text{ref}}, \tag{17}$$

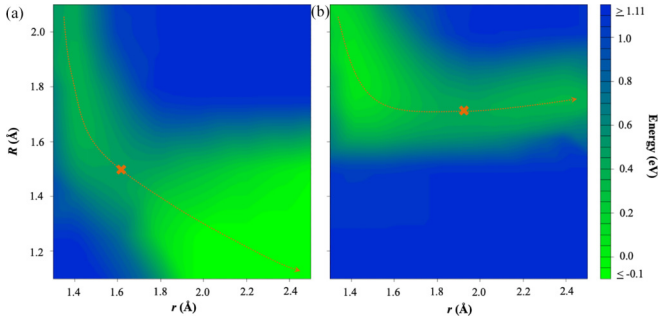

FIG. 4. Interaction energies $E_{\text{int}}(r, R)$ for (a) an oxygen molecule and a Pt catalyst surface and (b) an oxygen molecule and a M-Pt catalyst surface. The dotted orange line represents the trajectory of the oxygen molecule during the oxygen splitting reaction. The orange x marks the location of the activation barrier. Plots drawn using the AKIMA package for R [31].

where $E(r, R)$ is the energy of the slab + oxygen molecule system as obtained from a single-point DFT calculation. E_{ref} is a reference energy, which corresponds to the energy of the system when the catalyst and oxygen molecule are isolated from each other and not interacting. E_{ref} can be obtained as $E_{\text{ref}} = E_{\text{slab}} + E_{\text{Ox}}$, where E_{slab} is the energy of the slab in isolation and E_{Ox} is the energy of an isolated O_2 molecule with its equilibrium bond length $r = 1.2$ Å. These energies were computed for various bond lengths r between 1.2 Å and 2.5 Å, and various heights R between 1.1 Å and 2.1 Å using DFT as implemented in VASP, with spin polarization, the rev-vdW-DF2 exchange-correlation functional [30], a 450 eV basis set cutoff, and $3 \times 3 \times 2$ Γ-centered k-point grids. Note that Eq. (17) assumes that the structural relaxation rate of the surface is much slower than the O_2 dissociation rate.

A contour plot of the interaction energy is shown in Fig. 4. From these plots, the activation energy ϵ_i can be obtained by identifying the energy maximum along the lowest energy pathway between intact O_2 ($r = 1.2$ Å) and dissociated O_2 ($r = 2.1$ Å). In Fig. 4 the locations of the activation barriers are indicated by the orange crosses. The activation energies are calculated to be $\epsilon_{\text{Pt}} = 0.46$ eV and $\epsilon_{\text{M-Pt}} = 0.41$ eV. The small 0.05 eV decrease in activation energy for oxygen splitting indicates only a modest improvement in catalytic performance for M-Pt compared to Pt. Similar results were reported in Ref. [13], which considered a monolayer platinum catalyst on an iron substrate.

We now consider the price dynamics of M-Pt. As mentioned above, M-Pt plays the role of the product M and platinum as the commodity C. The price of platinum was simulated using a GARCH(1,1) + ARMA(1,1) time-series model fitted to the price of real platinum between 2016 and 2022 (see the Appendix). This time-series model includes a nonstationary noise term as well as a deterministic trend. Simulated platinum prices are expressed in units of decigrams so that they fluctuate over a similar range as the Gaussian commodity prices described in the previous section. For consistency we use the same choice of parameters as used in the previous section (Table II). These parameters are satisfactory for the present work, which focuses on how product characteristic improvements affect the transmission of commodity price fluctuations. Simulations are again performed using the Euler-Maruyama scheme, using the parameters shown in Table II. Because the GARCH(1,1) + ARMA(1,1) propagates in discrete time, and therefore cannot predict price changes over arbitrarily short intervals, we padded the sequence of predicted values using linear interpolation in order to use a small time step in our simulations.

TABLE II. Parameters used for the case of the platinum commodity. Symbols are defined in the text.

$p_M(0)$	0 USD/dg	v_a	0.75
c_1	0.1/day	v_b	0.75
c_2	100 USD/(dg day)	h	0.003 days
μ_a	1.0 dg/USD	n_{ts}	2366 days
μ_b	2.5	T	300 K

Figure 5(a) shows simulations of the M-Pt price $[p_M(t)]$ using the parameters shown in Table II. The M-Pt price is

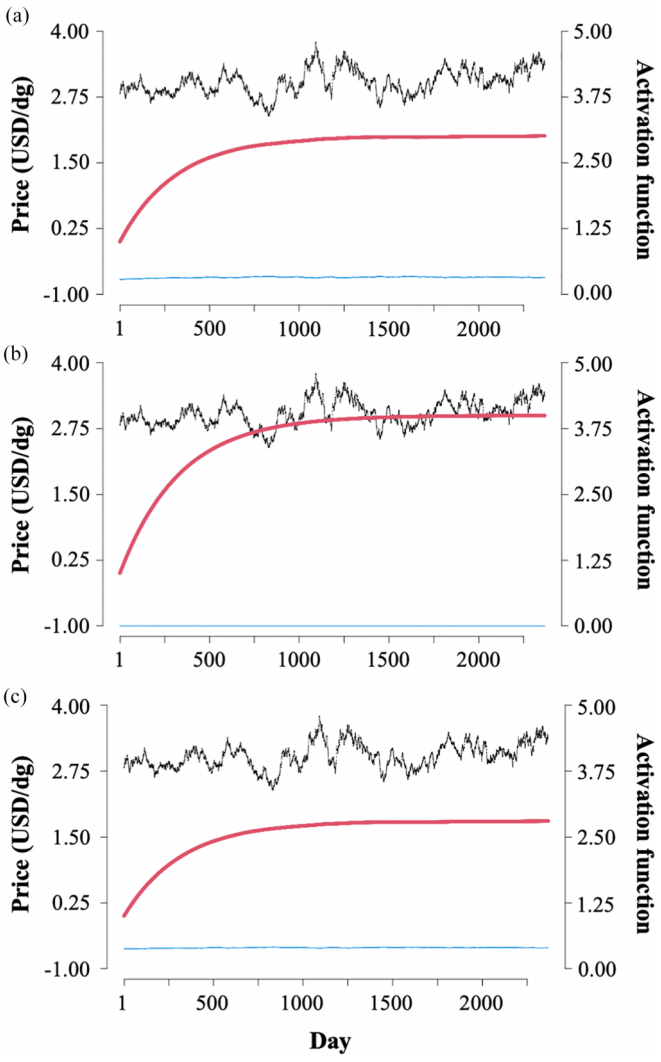

FIG. 5. Representative trajectories for the platinum commodity case. (a) Baseline case; (b) low consumer heterogeneity case ($v_a = 0.1$, $v_b = 0.1$); (c) high consumer heterogeneity ($v_a = 1.0$, $v_b = 1.0$). Unless otherwise mentioned, all parameters set as in Table II.

remarkably stable, following a smooth curve and not showing any fluctuations at all. This result is not surprising under this particular parameter regime. While the activation energies for oxygen splitting on M-Pt may be only 0.05 eV smaller compared to Pt, this corresponds to a log characteristic ratio of $Q = 1.93$, which is quite large. Moreover, the platinum price ($p_C(t)$, C = Pt) does not vary as wildly as the Gaussian prices shown in the previous section, at least when expressed in units decigrams. As a consequence, there are two factors operating to stabilize the input signal for the activation function: the large value of Q, which desensitizes the input signal to small changes in price differences, and the relatively steady value of $p_C(t)$, which prevents large price differences from occurring. The result is a steady input signal which samples the activation function over a very narrow range. This is reflected in the essentially flat blue curve in Fig. 5(a). As a consequence of the latter, the M-Pt price can be approximated by a differential equation of the form $dp_M/dt = -c_1 p_M + C$, where C is a constant, which describes a smoothly increasing curve which converges to a constant asymptotic value.

The results are much the same even for the cases of high and low consumer heterogeneity. Figure 5(b) shows the case of a consumer population with low heterogeneity ($v_a = 0.1$, $v_b = 0.1$). Almost exactly the same results are observed, which is expected on the basis of the reasoning above: while decreasing heterogeneity will change the shape of the activation function, making it more steplike in the region of the inflection point, this will not change the fact that the stable input signal will only be able to probe it over a very narrow range. In this case, the input signal continually samples the left-hand tail of the activation function, where its value is zero. Compared to the baseline case described above, this results in a larger value of the asymptotic M-Pt price. Similar remarks apply to the case of a consumer population with high heterogeneity [Fig. 5(c), $v_a = 1.0$, $v_b = 1.0$], where the flattened activation function means that the stable input signal continually samples a value near 0.5. Compared to the low-heterogeneity case, this lowers the asymptotic value of the M-Pt price.

These results suggest that, for certain consumer populations, small improvements in material properties can significantly suppress the transmission of commodity price fluctuations. However, these results need to be applied with care in the real world. Before committing to such applications, consumer surveys should be performed to estimate the values of the model parameters and to evaluate the validity of model assumptions (i–iv). Indeed, our simulations for the case of Gaussian commodities in the previous section show that low consumer heterogeneities can potentially enhance the transmission of commodity price fluctuations, which heightens the need for consumer population surveys in real-world applications of our theory.

IV. DISCUSSION

The model makes a number of assumptions which could be reconsidered in future work. In mainstream economics, utility functions similar to the one in Eq. (3) are often used for modeling consumer demand, particularly ones where product characteristics enter logarithmically and prices enter linearly [15]. There is little motivation for replacing these ingredients in our model at present. A more serious shortcoming of our model is the lack of an unobserved component in our utility functions; that is, the allowance for product characteristics which are important to the consumers but unknown to the modeler. We have ignored this here because the unobserved component needs to be correlated with price, which significantly complicates subsequent analysis. Our utility functions also ignored consumer budget constraints, as well as the possibility of a third option where consumers choose to purchase neither item. Proper consideration of these two factors would be interesting for further work, and may introduce new factors which modulate the transmission of commodity price fluctuations.

While an Ornstein-Uhlenbeck processes was selected as a generic stochastic process for commodity price evolution in Sec. III A, Gaussian commodity fluctuations are not essential to our price dynamics model. It is important to emphasize this point, as careful studies of real commodity price fluctuations have shown that their distributions are often heavy tailed [32]. The conclusions in Sec. III A (which are the main econophysics-related conclusions of this paper) were obtained entirely by considering the "neuron"-type model representation shown in Fig. 1. These conclusions are (i) small log characteristic ratios Q will enhance the transmission of commodity price fluctuations to product prices, and conversely for large ratios [Figs. 2(b) and 2(c)]; (ii) low consumer heterogeneity will enhance the transmission of commodity price fluctuations to product prices, and conversely for high consumer heterogeneity [Fig. 2(e)]; and (iii) suppression of commodity price fluctuations by product characteristics requires sufficient consumer heterogeneity [Fig. 2(f)]. These conclusions were obtained by considering how the input signal ($\Delta p/Q$ in Fig. 1) sweeps over the transition region of the neuron activation function, as well as the effect of consumer population parameters on the width of the transition region. No assumptions on the distribution of commodity price fluctuations were needed to reach (i)–(iii), meaning that they hold even if realistic heavy-tailed models for commodity prices are used.

Another important point concerns our assertion that p_M represents the actual price of the product. This assertion is acceptable within the confines of this study, however in general the connection between the p_M in our model and product prices can be complicated. From a microeconomics perspective, the price of the product M would emerge as a result of iterative price-setting games between suppliers. On the other hand, econophysics research usually assumes a dynamical equation such as Eq. (1) from the outset. A connection between these two approaches might be made by assuming that the suppliers of M set their prices within a very short time, and that consumers make their selections of M or C over a much longer timescale. We could then consider a short time interval $(t, t + \delta t)$ over which the demand for M is essentially constant. We might then imagine Bertrand-type competition arising between suppliers during this interval as they try to attract the consumers who which to purchase a unit of M. If the market price of M happened to be $p_M(t)$ at the start of this interval, then by the end of the interval it would be reduced to $p_M(t) - \epsilon$, where ϵ could be made

small by sending δt to zero. If the limiting value of ϵ could be shown to be proportional to $S_M - D_M$, then a connection between the microeconomics and econophysics approaches would be established and the conditions under which p_M represents product price would become clearer. This argument is obviously idealized, as it is hard to justify why price setting by suppliers and choice formation by consumers would take place on such vastly different timescales. The Bertrand model is known to be flawed as well. In realistic situations, the product price would probably emerge as some kind of composite of p_M [as given by Eq. (1)] and other kinds of "correction" factors. It would therefore be inaccurate to speak of the transmission of commodity price fluctuations to product prices in the general case. Rather, it would be more correct to speak of the transmission of commodity price fluctuations to one component of the overall product price.

Of particular interest to econophysics are assumptions related to correlation and memory. Our model treats consumers as independent "Markovian" agents who are neither influenced by other agents nor have any memory of past events. The former shortcoming could be overcome by replacing the utility expression in Eq. (3) with something resembling a Ising Hamiltonian expression, where an interaction term is included to encourage or discourage consumers from mimicking the choices of others. Such Ising-type models are widely used in social physics [33–36]. The inclusion of a consumer-level interaction term would certainly affect how commodity price fluctuations are transmitted to product prices. On the other hand, the inclusion of memory effects at the level of consumers looks more difficult. One indirect approach might be to impose a waiting period between the selection times of each consumer, and allowing the waiting period to depend upon the most recent selection. The waiting time distribution might then affect the transmission of commodity price fluctuations. Such an approach would still be Markovian in the strictest sense of the word, but may introduce memory effects in a similar way as a formally non-Markovian model would. Other memory effects arising at the macroscopic level of prices could be included by use of fractional calculus and other emerging econophysics techniques [37].

This paper finished by considering a concrete example where a monolayer catalyst competes with a pure platinum catalyst. The inclusion of this example was not contrived. On the contrary, we wish to expand the remit of materials science to include questions related to price stability and marketplace competitiveness. This paper has taken only a baby step in this direction. Indeed, future work in this direction will require us to use survey data to characterize real-world markets and consumer attitudes towards material characteristics and price. As presented here, this work simply shows that under the right market conditions, material properties can have a profound modulating effect on the fluctuations which ripple through the price system. The fact that physicists have powerful and mature tools at their disposal for computing material properties puts them in a unique position to study this area in detail.

V. CONCLUSIONS

The transmission of fluctuations between the prices of products is an important aspect of real-world price dynamics, but the factors which modulate such transmissions are poorly understood. In this paper we presented a model for the price of a product which competes directly with a commodity in a specific market. By aggregating the choices of individual consumers, we found that commodity price fluctuations transmit to the price of the product by way of a sigmoidal activation function, similar to the ones which appear in studies of neuron dynamics. Importantly, we identified the role of product characteristics in modulating the transmission of commodity price fluctuations: high log characteristic ratios between the product and commodity tend to suppress the transmission of commodity price fluctuations, and low log characteristic ratios tend to enhance the transmission. This point was confirmed in numerical simulations, which showed a dramatic reduction in product price fluctuations for large values of the log characteristic ratio. On the other hand, these simulations demonstrated that such desensitization to commodity price fluctuations is dependent upon the state of the market. In particular, such desensitization might not occur when the consumer population is highly homogeneous in its attitudes towards product characteristics and price.

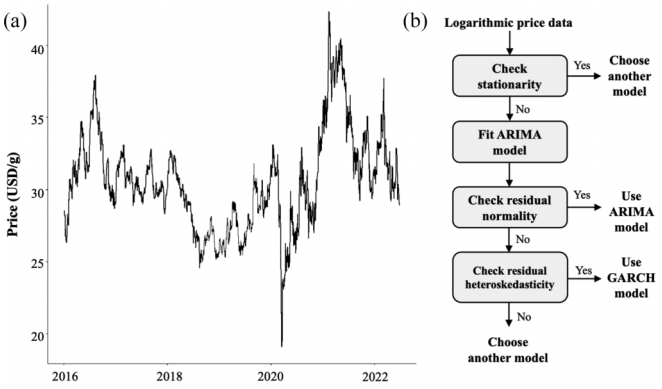

FIG. 6. Time-series data for the price of platinum. Data obtained from Ref. [38]. Flow diagram for fitting time-series model.

ACKNOWLEDGMENTS

This work was supported by K. Matsushita Foundation Grant No. 21-G09, the Sompo Environment Foundation, Japan Society for the Promotion of Science Kakenhi Grants No. 18K14126, No. 19H04574, and No. 21K05003, and internal funding from the Graduate School of Advanced Integrated Studies in Human Survivability and the Institute for Integrated Cell-Material Sciences at Kyoto University.

APPENDIX

Platinum prices were simulated using a time-series model. This mode was fit to the real price of platinum recorded during the period January 1, 2016, to July 1, 2022 [see Fig. 6(a)] (data source: [38]). The time-series model was built in a stepwise manner according to the scheme in Fig. 6(b). In the following, we let y_t denote the price of platinum at time t and $z_t = \ln y_t$. All hypothesis tests and model parameter estimations were performed within the R statistical environment. In the first step, the KPSS test was used to determine

whether z_t possessed a unit root. We were able to reject the null hypothesis that there is no unit root (test statistic = 2.32), suggesting that z_t is not stationary. The KPSS test was performed with the function ur.kpss in the package TSERIES [39]. In the second step, we attempted to fit an ARIMA model to the time series z_t. The model which minimized the AIC (Akaike Information Criterion) was an ARIMA(0,1,0) model, which is equivalent to a random walk with Gaussian-distributed steps. In order to confirm whether this is an appropriate model for z_t, a Jarque-Bera test was conducted. The null hypothesis (that $z_t - z_{t-1}$ is normally distributed) was rejected (P value $<2.2 \times 10^{-16}$). Based on this result, we reject the ARIMA(0,1,0) model as a model for z_t. Finally, we conducted the Breusch-Pagan test to check for heteroskedasticity. The null hypothesis [homoskedasticity in the residuals of z_t with respect to the ARIMA(0,1,0) model above] was rejected (P value $= 9.5 \times 10^{-4}$), suggesting heteroskedasticity in the time series z_t. The ARIMA model was fit using the function arima with the package STATS. The Jarque-Bera test was performed using the function arque.bera.test in the package TSERIES. The Breusch-Pagan test was performed using the function bptest in the package LMTEST [40].

The presence of heteroskedasticity suggests that we fit a GARCH(p, q) model to z_t. The GARCH(p, q) model has the form $r_t = \mu + \epsilon_t$, where $E(\epsilon_t^2|F_{t-1}) = \sigma_t^2$,

$$\sigma_t^2 = \omega + \sum_{i=1}^{p} \alpha_t \epsilon_{i-1}^2 + \sum_{i=1}^{q} \beta_i \sigma_{i-1}^2, \tag{18}$$

and F_{t-1} denotes the sigma field generated by ϵ_j, $j = 0, \ldots, t-1$. In the third step, a GARCH(1,1) model fitted to z_t resulted in $\mu = 6.85$ (P value $= 0$), $\omega = 1.33 \times 10^{-4}$ (P value $= 1.0 \times 10^{-6}$), $\alpha_1 = 0.89$ (P value $= 0$), and $\beta_1 = 0.10$ (P value $= 8.17 \times 10^{-3}$). This model achieved an AIC of -2.77. Finally, a GARCH(1,1) + ARMA(1,1) model was fit to z_t, resulting in $\mu = 6.79$ (P value $= 0$), $\omega = 1.0 \times 10^{-6}$ (P value $= 0.34$), $\alpha_1 = 3.5 \times 10^{-2}$ (P value $= 0$), $\beta_1 = 0.96$ (P value $= 0$), an autoregression parameter of 0.99 (P value $= 0$), and a moving average parameter of 1.77×10^{-2} (P value $= 0.46$). This model achieved an AIC of -5.75. While the GARCH(1,1) + ARMA(1,1) model contained two statistically insignificant parameters, we opted to use it over the simpler GARCH(1,1) model because its simulated sample paths appeared to resemble the original platinum price data (y_t) when exponentiated and plotted. These models were fit using the functions ugarchspec and ugarchfit in the package RUGARCH [41].

[1] K. Anand and J. Khedair, and R. Kuhn, Structural model for fluctuations in financial markets, Phys. Rev. E **97**, 052312 (2018).

[2] E. Scalas, The application of continuous-time random walks in finance and economics, Physica A **362**, 225 (2006).

[3] J.-C. Li, M.-Z. Xu, X. Han, and C. Tao, Dynamic risk resonance between crude oil and stock market by econophysics and machine learning, Physica A **607**, 128212 (2022).

[4] G. Poitras, The pre-history of econophysics and the history of economics: Boltzmann versus the marginalists, Physica A **507**, 89 (2018).

[5] A. R. Bosco de Magalhaes, Wealth dynamics in a market with information asymmetries, Phys. Rev. E **107**, 014305 (2023).

[6] S. M. Krause, S. Borries, and S. Bornholdt, Econophysics of adaptive power markets: When a market does not dampen fluctuations but amplifies them, Phys. Rev. E **92**, 012815 (2015).

[7] N. Johnson and B. Tivnan, Mechanistic origin of dragon-kings in a population of competing agents, Eur. Phys. J. Spec. Top. **205**, 65 (2012).

[8] J-P. Onnela, A. Chakraborti, K. Kaski, J. Kertesz, and A. Kanto, Dynamics of market correlations: Taxonomy and portfolio analysis, Phys. Rev. E **68**, 056110 (2003).

[9] W. Shi and P. Shang, Cross-sample entropy statistic as a measure of synchronism and cross-correlation of stock markets, Nonlinear Dyn. **71**, 539 (2013).

[10] J. Letzelter, J. B. Hill, and H. Hacquebord, An overview of skin antiseptics used in orthopaedic surgery procedures, J. Am. Acac. Orthop. Surg. **27**, 599 (2019).

[11] I. V. Kirillina, L. A. Nikiforov, A. A. Okhlopkova, S. A. Sleptsova, C. Yoon, and J.-H. Cho, Nanocomposites based on polytetrafluoroethylene and ultrahigh molecular weight polyethylene: A brief review, Bull. Korean Chem. Soc. **35**, 3411 (2014).

[12] T. Wang, K. S. Chen, J. Mishler, S. C. Cho, and X. C. Adroher, A review of polymer electrolyte membrane fuel cells: Technology, applications, and needs on fundamental research, Appl. Energy **88**, 981 (2011).

[13] M. C. S. Escano, T. Kishi, S. Kunikata, H. Nakanishi, and H. Kasai, Pt monolayer on Fe(001) catalyst for O_2 reduction: A first principles study, e-J. Surf. Sci. Nanotechnol. **5**, 117 (2007).

[14] K. J. Lancaster, A new approach to consumer theory, J. Polit. Econ. **74**, 132 (1966).

[15] S. Berry, J. Levinsohn, and A. Pakes, Automobile prices in market equilibrium, Econometrica **63**, 841 (1995).

[16] P. Bajari and C. K. Benkard, Demand estimation with heterogeneous consumers and unobserved product characteristics: A hedonic approach, J. Polit. Econ. **113**, 1239 (2005).

[17] R. C. Feenstra, Exact hedonic price indexes, Rev. Econ. Stat. **77**, 634 (1995).

[18] J. J. Hopfield, Neurons with graded response have collective computational properties like those of two-state neurons, Proc. Natl. Acad. Sci. USA **81**, 3088 (1984).

[19] R. Kuhn and S. Bos, Statistical mechanics for neural networks with continuous-time dynamics, J. Phys. A.: Math. Gen. **26**, 831 (1993).

[20] Y. Tanimura, Stochastic Liouville, Langevin, Fokker–Planck, and master equation approaches to quantum dissipative systems, J. Phys. Soc. Jpn. **75**, 082001 (2006).

[21] E. Díaz-Francés and F. J Rubio, On the existence of a normal approximation to the distribution of the ratio of two independent normal random variables, Stat. Pap. **54**, 309 (2013).

[22] A. Nevo, Measuring market power in the ready-to-eat cereal industry, Econometrica **69**, 307 (2001).

[23] D. T. Gillespie, Exact numerical simulation of the Ornstein-Uhlenbeck process and its integral, Phys. Rev. E **54**, 2084 (1996).
[24] Dassault Systems BIOVIA, Materials studio 2020 (2020).
[25] K. Burke, Perspective on density functional theory, J. Chem. Phys. **136**, 150901 (2012).
[26] A. Pribram-Jones, D. A. Gross, and K. Burke, Dft: A theory full of holes, Annu. Rev. Phys. Chem. **66**, 283 (2015).
[27] S. Yotsuhashi, Y. Yamada, W. A. Dino, H. Nakanishi, and H. Kasai, Dependence of oxygen dissociative adsorption on platinum surface structures, Phys. Rev. B **72**, 033415 (2005).
[28] G. Kresse and J. Furthmuller, Efficient iterative schemes for *ab initio* total energy calculations using a plane-wave basis set, Phys. Rev. B **54**, 11169 (1996).
[29] J. P. Perdew, K. Burke, and M. Ernzerhof, Generalized gradient approximation made simple, Phys. Rev. Lett. **77**, 3865 (1996).
[30] I. Hamada, Van der Waals density functional made accurate, Phys. Rev. B **89**, 121103(R) (2014).
[31] H. Akima, A. Gebhardt, T. Petzold, and M. Maechler, akima: Interpolation of irregularly and regularly space data (2022), https://cran.r-project.org/web/packages/akima/index.html.
[32] M. Watorek, J. Kwapien, and S. Drozdz, Financial return distributions: Past, present, and COVID-19, Entropy **23**, 884 (2021).
[33] C. H. Lee and A. Lucas, Simple model for multiple-choice collective decision making, Phys. Rev. E **90**, 052804 (2014).
[34] M. Löwe, K. Schubert, and F. Vermet, Multi-group binary choice with social interaction and a random communication structure—A random graph approach, Physia A: Stat. Mech. Appl. **556**, 124735 (2020).
[35] S. Nakayama and Y. Nakamura, A fashion model with social interaction, Physia A: Stat. Mech. Appl. **337**, 625 (2004).
[36] C. Castellano, S. Fortunato, and V. Loreto, Statistical physics of social dynamics, Rev. Mod. Phys. **81**, 591 (2009).
[37] V. E. Tarasov, Fractional econophysics: Market place dynamics with memory effects, Physia A: Stat. Mech. Appl. **557**, 124865 (2020).
[38] Platinum futures (PLF3) daily price data, https://www.investing.com/commodities/platinum.
[39] A. Trapletti, K. Hornik, and B. LeBaron, tseries: Time series analysis and computational finance (2022), https://cran.r-project.org/web/packages/tseries/index.html.
[40] T. Hothorn, A. Zeileis, R. W. Farebrother, C. Cummins, G. Millo, and D. Mitchell, lmtest: Testing linear regression models (2022), https://cran.r-project.org/web/packages/lmtest/index.html.
[41] A. Galanos and T. Kley, rugarch: Univariate GARCH models (2022), https://cran.r-project.org/web/packages/rugarch/index.html.